A Case Study of the Great Plains Low-Level Jet Using Wind Profiler Network Data and a High Resolution Mesoscale Model

S. Zhong, J. D. Fast, X. Bian, S. Stage, and C. D. Whiteman
Pacific Northwest National Laboratory
Richland, Washington

Introduction

The Great Plains low-level jet (LLJ) has important effects on the life cycle of clouds and on radiative and surface heat and moisture fluxes at the Atmospheric Radiation Measurement (ARM) Southern Great Plains (SGP) Cloud and Radiation Testbed (CART) site. This diurnal phenomenon governs the transport and convergence of low-level moisture into the region and often leads to the development of clouds and precipitation. A full understanding of the life cycle of clouds at the SGP CART site and their proper representation in single column and global climate models cannot be obtained without an improved understanding of this important phenomenon.

A detailed case study of one complete episode of a typical summertime LLJ using data collected by the National Oceanic and Atmospheric Administration (NOAA) wind profiler demonstration network and soundings released at the CART central facility is presented. A two-day period beginning on the morning of 11 July 1992 and ending on the morning of 13 July 1992 was chosen for this study because a typical summertime LLJ was evident over many of the observational sites. The high temporal and spatial resolution of the data permits a much more detailed picture of the Great Plains LLJ and its associated mesoscale convective systems than is possible from previous studies. A three-dimensional mesoscale numerical model is also used to simulate the episode and to provide information on the physical mechanisms responsible for the initiation, evolution, maintenance, and decay of the LLJ. The model is also used to examine the sensitivity of the LLJ to various factors such as the beta effect, soil moisture content and distribution, and the possible feedbacks from cloud and precipitation processes.

Data

The data used in this study are vertical wind profiles from the wind profiler demonstration network and temperature and moisture soundings at the central facility. The profiler network consists of 31 stations mostly scattered across the southern and central Great Plains. Each wind profiler provides hourly vertical profiles of horizontal wind components. The geographic location of this profiler network (Figure 1) and the high temporal resolution of the wind profile measurements make it ideal for depicting the spatial variation and the diurnal evolution of the LLJs.

Model

The model used for the case study is the Colorado State University Regional Atmospheric Modeling System (RAMS) (Pielke et al. 1992). A nested grid configuration was used with a coarse grid of 100-km resolution covering most of the United States, including the Gulf of Mexico, and a fine grid of 25-km resolution covering most of the Great Plains. Thirty vertical levels were used for both grids. The simulation was initialized at 0600 CST,

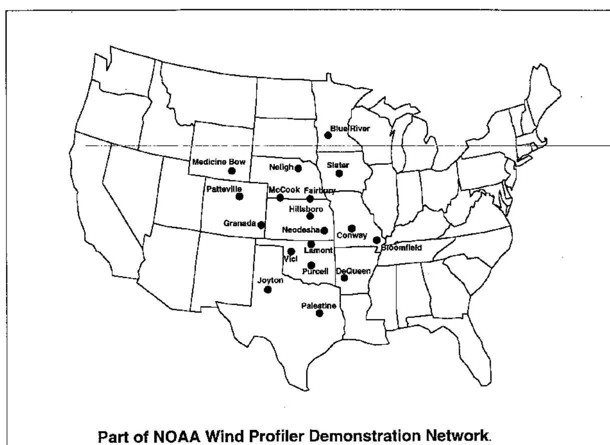

Figure 1. Locations of the wind profilers used for the present study in the NOAA wind profiler demonstration network. The SGP CART central facility is located at Lamont, Oklahoma.

11 July, using data from the National Meteorological Center global analysis, standard rawinsonde observations, wind profiles from the profiler network, and special soundings from the central facility. The simulation continued for 48 hours during which the lateral and the top boundary conditions were allowed to change by "nudging" the outermost nodes at these boundaries towards the objectively analyzed observational fields that were available every 12 hours.

Model Verification

The model's performance in simulating the LLJ in this case is evaluated by the observations. Figure 2 shows the comparison of the horizontal wind vectors at the height of the LLJ maximum at the time of maximum LLJ development. Very good agreement was obtained between the simulated and observed position of the jet core, the width of the jet core, the values of the wind maximum, as well as the associated wind shear and vorticity fields. A good agreement is also reached between simulated and observed precipitation fields, as shown in Figure 3. The maximum precipitation occurs at the leading edge of the jet due to low-level moisture convergence and strong upward motion produced by the LLJ. These comparisons suggest that the model is able to capture the principal features of the LLJ and associated vertical motion and precipitation fields, which justifies the use of the model for an in-depth analysis as presented below.

Momentum Balance Analysis

Because the model produces a dynamically balanced data set, it can be used to examine the forces that make up the individual components of the momentum equation. These forces control the momentum balance and, hence, account for spatial and temporal variations of the wind field.
The horizontal momentum equation can be written as

$$\frac{\partial \vec{v}}{\partial t} = \underbrace{-\vec{v} \bullet \nabla \vec{v}}_{\text{I}} \underbrace{- \alpha \nabla p}_{\text{II}} \underbrace{- 2\vec{\Omega} \times \vec{v}}_{\text{III}} \underbrace{+ \alpha \vec{F}}_{\text{IV}} \qquad (1)$$

This equation states that wind accelerations are driven by the balance between horizontal advection (term I), pressure gradient force (term II), Coriolis force (term III), and friction (term IV).

The diurnal evolution of the individual momentum equation terms shows similar patterns at stations within the jet core. An example is shown in Figure 4 for Lamont, Oklahoma. Clearly, within the jet core, the momentum balance is determined predominantly by the pressure

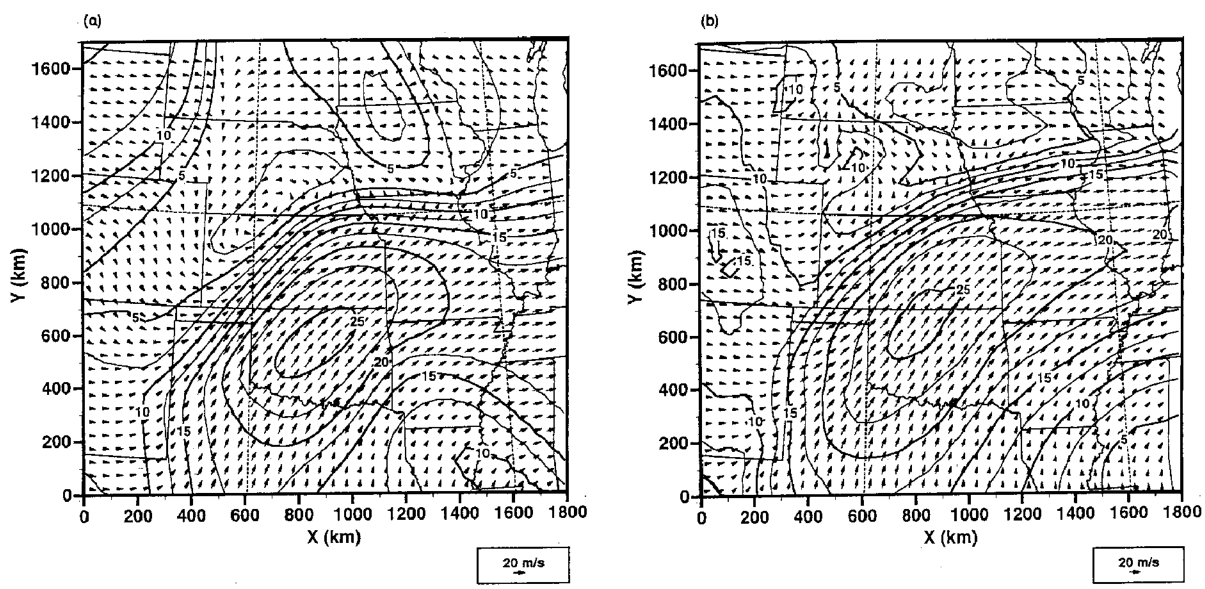

Figure 2. Observed (left) and simulated (right) wind speed contours and vector fields at 867 m at 0200 CST, 13 July 1992.

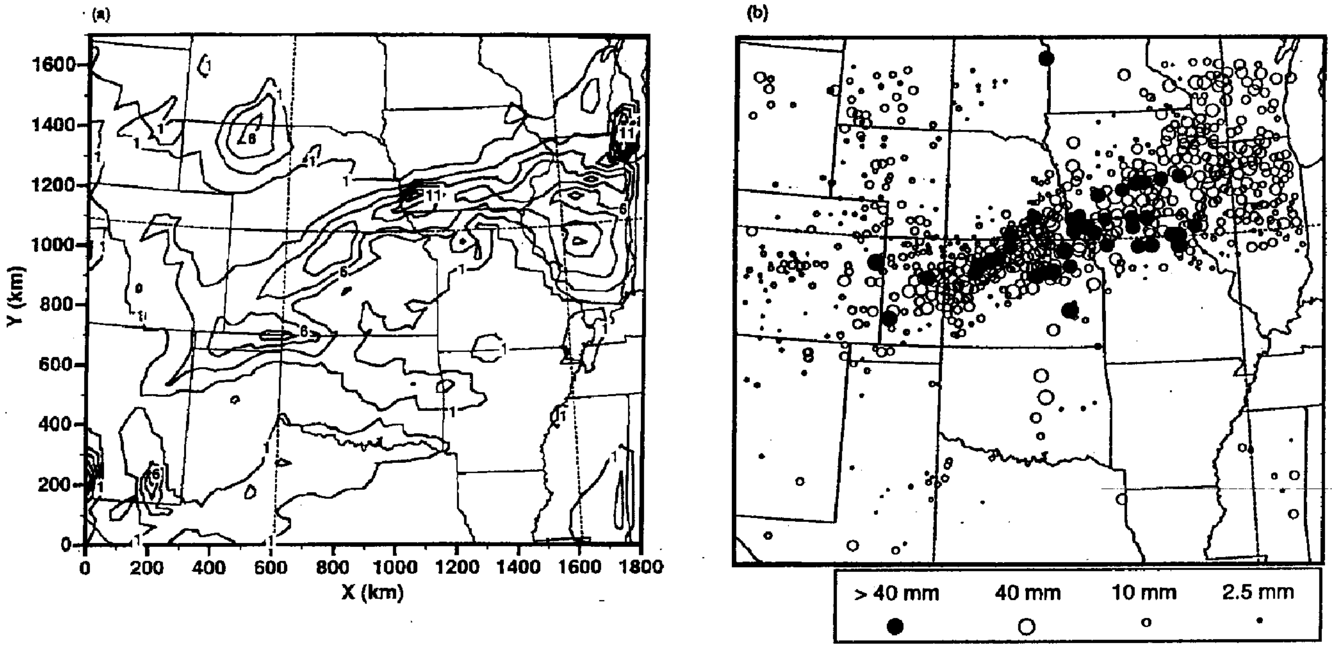

Figure 3. Simulated (a) and observed (b) 24-h total surface precipitation (in mm) ending at 0600 CST, 13 July. The solid circles indicate total precipitation greater or equal to 10 mm, the open circles indicate total precipitation between 1 mm to 10 mm, and the x indicates precipitation amount less than 1 mm.

gradient force, Coriolis force, and friction during daytime, and by the pressure gradient and Coriolis forces during nighttime. The Coriolis force shows a strong diurnal oscillation, which, together with the diurnal oscillation of friction, accounts for most of the diurnal variation of total acceleration in the jet core. The pressure gradient force, on the other hand, shows a relatively small diurnal variation. This implies that frictional decoupling and inertial oscillation, as proposed by Blackadar (1957), are the primary mechanisms responsible for the diurnal variation of the LLJ. The terrain-induced pressure gradient oscillation over the sloping Great Plains appears to be less significant than was suggested in previous studies (Holton 1967). This is consistent with the analysis of ageostrophic wind components, which indicates that the isallobaric components arising from the changes in horizontal pressure gradients are secondary to the inertial components associated with the turning of the wind by the Coriolis force in the total ageostrophic wind.

In contrast to the stations within the jet core, stations west of the jet core, as represented by Platteville, Colorado in Figure 4, display strong diurnal oscillations of the pressure gradient force, especially in the u-momentum component, reflecting the effect of diabatic cooling and heating above the sloping terrain. Nevertheless, the pressure gradient force, or the geostrophic wind, is much smaller than at locations within the jet core. By examining the differences in pressure gradient force between the two stations in Figure 4, one can see that the pressure gradient force is considerably

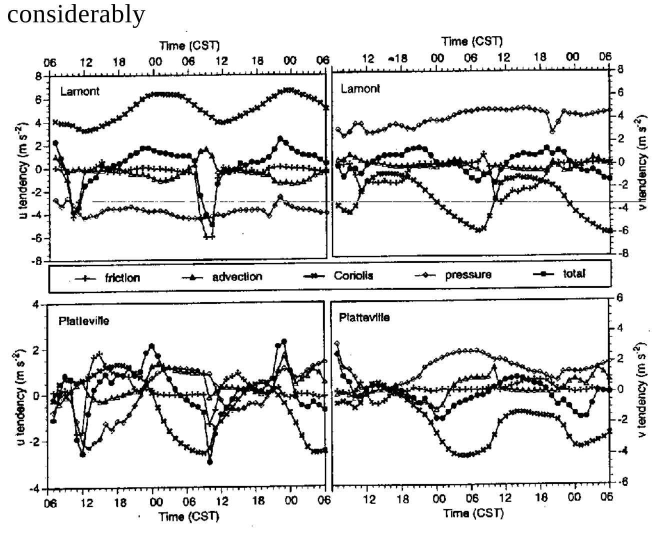

Figure 4. Time variation of the individual terms in the horizontal momentum equation at 867-m mode level at two stations. The time starts from 0700 CST, 11 July and ends at 0600 CST, 13 July.

smaller outside the jet core than inside. This suggests that a strong synoptic-scale pressure gradient is crucial for the the formation of a strong LLJ. Without such a large-scale pressure gradient, or the "basic flow" on which the frictional stress could operate diurnally, there would not be the strong diurnal LLJ that is so characteristic of the Great Plains.

Sensitivity Studies

Sensitivity tests were conducted to study the relative influence of various physical factors on LLJ characteristics. Simulations with a constant Coriolis parameter in the entire domain, as compared to the actual situation in which the Coriolis parameter varies meridionally, result in a weaker jet, confirming Wexler's (1961) prediction that the increase of Coriolis parameter with latitude enhances the LLJ. Simulations with different soil moisture values show that changes in soil moisture have little effect on the phase of the diurnal oscillation of the jet, but modify the amplitude of the oscillation with larger amplitudes associated with drier soil (Figure 5). However, considerably larger vertical velocities at the leading edge of the jet are found to be associated with wet soil than with dry soil. This enhancement of rising motions appears to be associated with latent heat release from precipitation; the simulation without cloud and precipitation processes displays much weaker rising motions ahead of the jet than the experiment retaining the processes.

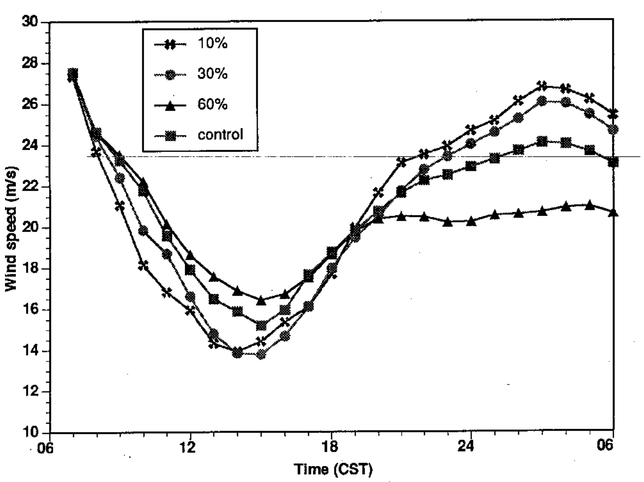

Figure 5. Time variation of maximum wind speeds averaged over the 698-, 867-, 1071-m model vertical levels from 0700 CST, 12 July, to 0600 CST, 13 July, for simulations with different soil moisture contents. The control simulation uses a realistic soil moisture distribution derived from the crop moisture index.

Summary

A combined analysis and modeling approach has produced a detailed description of the three-dimensional structure of the LLJ and its time evolution. Relative contributions to the boundary-layer wind oscillation from different forces were diagnosed by reconstructing tendency terms in the momentum equations. The analyses suggest that the diurnal oscillation of horizontal pressure gradient over sloping terrain is secondary to the inertial oscillation mechanism resulting from the release of frictional constraint in the evening and throughout the night in driving the LLJ. Sensitivities of the LLJ to the beta effect, soil moisture content and distribution, and cloud and precipitation feedbacks were also investigated. The meridional variation of the Coriolis parameter as air moves northward appears to enhance the strength of the jet. A larger amplitude of the diurnal oscillation of the jet speed is found to be associated with drier soil, while rising motion at the leading edge of the jet is stronger for wetter soil. This enhanced vertical motion appears to be associated with latent heat release due to precipitation.

The results suggest that an improved turbulence treatment and an incorporation of information such as soil moisture are likely to improve the ability of forecast models and global climate models in simulating the LLJ and the associated nocturnal convection. Research has also demonstrated the ability of radar wind profilers to improve our understanding of a well-studied boundary-layer phenomenon. More wind profilers are now equipped with radio-acoustic sounding systems which allow vertical profiles of virtual temperatures to be measured as well. Observations from these profilers will provide a great opportunity to verify previous conceptions regarding the forcing of the LLJ.

References

Blackadar, A. K. 1957. Boundary layer wind maximum and their significance for the growth of nocturnal inversions, *Bull. Amer. Met. Soc.*, **38**, 283-290.

Holton, J. R. 1967. The diurnal boundary layer wind oscillation above sloping terrain, *Tellus*, **19**, 199-205.

Pielke, R. A., W. R. Cotton, R. Walko, C. J. Tremback, W. A. Lyons, L. D. Grasso, M. E. Nicholls, M. D. Moran, D. A. Wesley, T. J. Lee, and J. H. Copeland. 1992. A comprehensive meteorological modeling system - RAMS, *Meteor. Atmos. Phys.*, **49**, 69-91.

Wexler, H. 1961. A boundary layer interpretation of the low level jet, *Tellus*, **13**, 368-378.